FTY720 attenuates LPS-induced acute lung injury through PP2A- tristetraprolin–dependent anti-inflammatory signaling

Keywords
Acute lung injury, Protein phosphatase 2, Tristetraprolin, Fingolimod hydrochloride, Inflammation

Abstract

Introduction
Acute lung injury (ALI) is characterized excessive inflammatory signaling and uncontrolled cytokine production. Tristetraprolin (TTP) is a key post-transcriptional regulator of inflammatory cytokines that negatively regulates inflammatory pathways. PP2A emerges as an important player to activate TTP. However, whether pharmacological activation of PP2A can restore TTP activity and thereby attenuate ALI remains unexplored.

Material and methods
A lipopolysaccharide (LPS)-induced mice model of ALI and LPS-stimulated RAW264.7 macrophages were used to evaluate the effects of FTY720 or siRNA PP2A. Lung injury and inflammation were assessed by histopathology, wet-to-dry weight ratio, bronchoalveolar lavage fluid analysis, and cytokine quantification. PP2A activity, p38 MAPK and TTP phosphorylation, and gene expression were analyzed using phosphatase assays, Western blot, ELISA, and quantitative RT-PCR.

Results
Pretreatment of FTY720, a well-established PP2A activator, significantly alleviated LPS-induced lung injury, inflammatory cell infiltration, and inflammatory cytokines release in vivo. Treatment with PP2A siRNA blocked the improvement effect induced by FTY720 in LPS-induced lung injury mice. LPS exposure significantly impaired PP2A activity without altering PP2A protein abundance, whereas FTY720 restored PP2A activity in lung tissues. Mechanistically, PP2A activation suppressed p38 MAPK phosphorylation and/or promoted dephosphorylation of TTP in LPS-induced macrophages. Moreover, PP2A activation by FTY720 inhibited p38 MAPK and TTP phosphorylation without affecting TTP transcription, leading to reduced inflammatory cytokine production.

Conclusions
Our findings demonstrate that PP2A activation blocked inflammatory responses by reprogramming the TTP activity. Pharmacological targeting of PP2A may represent a promising strategy for the treatment of acute lung injury.

1. Introduction

Acute lung injury (ALI) and acute respiratory distress syndrome (ARDS) remain major causes of morbidity and mortality worldwide, with limited effective pharmacological interventions. ALI/ARDS is characterized by alveolar capillary barrier dysfunction, leading to pulmonary edema, impaired gas exchange, and respiratory failure [1]. Despite advancements in supportive therapeutic techniques, targeted drugs addressing the core pathological mechanisms remain absent, highlighting the urgency of gaining a deeper understanding of disease mechanisms and developing novel therapeutic strategies.

Clinical evidence indicates that uncontrolled inflammatory responses are the primary drivers of tissue damage and disease progression. In particular, excessive production of inflammatory cytokines such as tumor necrosis factor-α (TNF-α), interleukin-1β (IL-1β), and interleukin-6 (IL-6), amplifies leukocyte recruitment, disrupts endothelial and epithelial integrity, and forms positive feedback loops that perpetuate and worsen the inflammatory response in the lungs [2-4]. Therefore, targeting the dysregulated inflammatory cascade, particularly at the level of cytokine production, has emerged as a core strategy for treating ALI.

Post-transcriptional control of cytokine expression has emerged as a critical checkpoint in blocking inflammatory responses. Tristetraprolin (TTP), a zinc-finger RNA-binding protein, is identified as a key mediator in this process by binding to the AU-rich elements (AREs) within the 3'-translated region (3'-UTR) of mRNAs encoding several key inflammatory cytokines, thereby promoting targeting mRNA degradation [5]. Genetic and functional studies have established TTP as a potent endogenous brake on inflammatory pathology [6]. It has also been reported that, in ALI, dysregulation of TTP activity is

implicated in excessive cytokine accumulation and inflammatory cell infiltration, suggesting that TTP represents a critical molecular node linking inflammatory signaling to disease severity [7].

The anti-inflammatory activity of TTP is tightly governed by post-translational modifications, most notably phosphorylation. Phosphorylation of TTP by stress-activated kinases such as p38 MAPK renders the protein functionally inactive. In contrast, dephosphorylation restores mRNA-destabilizing activity of TTP, thereby accelerating the resolution of inflammation [8]. However, direct inhibition of p38 MAPK has not increased the level of non-phosphorylated TTP, underscoring the complexity of upstream regulatory networks [9]. Recently, PP2A was identified as a major serine/threonine phosphatase capable of dephosphorylating components of the MAPK pathway as well as TTP itself, representing a potentially efficient and physiologically relevant pathway for inhibiting inflammatory responses in ALI [10]. This suggests that the PP2A-TTP axis may represent a potential endogenous regulatory pathway for inhibiting uncontrolled inflammatory responses in ALI.

FTY720, a compound synthesized from the metabolic products of the fungus Cordyceps sinensis, has been demonstrated in multiple studies to be a pharmacological activator of PP2A [11,12]. It can restore PP2A enzyme activity by binding to its endogenous inhibitory protein SET or the scaffold subunit PPP2R1A [11]. In inflammatory models, FTY720-mediated reactivation of PP2A has been shown to effectively inhibit the production of pro-inflammatory cytokines, providing a pharmacological basis for its anti-inflammatory effects [12,13]. However, whether FTY720 exerts protective effects in ALI through the PP2A-TTP axis remains unclear. This study focuses on verifying

whether FTY720 reduces LPS-induced lung injury by activating PP2A and promoting TTP dephosphorylation.

2. Materials and methods

Animals

Male C57BL6 mice (6–8 weeks old, 20–22 g) (Since the estrous cycle of female mice was a complex variable that was difficult to control and could interfere with the standardization of experiments, only male mice were selected for this study) were purchased from Experimental Animal Center of Xi'an Jiao Tong University and housed under specific pathogen–free conditions (25 ± 1.5 ºC; 65%±4% humidity; 12 h light-dark cycle). All experimental procedures were approved by the Medical Animal Research Ethics Committee of Xi'an Jiao Tong University.

Sample size estimation

According to the Pathological damage scores of lung tissues reported in the reference [14] (LPS group: 11.00 ± 0.82, FTY720 group: 7.20 ± 0.84), using G-power software (v.3.1.9.7), we calculated a sample size of 3 per group to achieve a power of 0.95 and an alpha error of 0.05. Considering a 20% dropout rate, 4 mice per group were required. Since this study required experiments such as histology, ELISA, and Western blotting, 10 mice per group were taken.

Grouping of experimental animals

Mice were randomly divided into 5 groups (n = 10 per group) according to simple randomization using a random number table in SPSS 26 (SPSS Inc., Chicago, IL, USA): control group (Con), LPS-induced ALI group (LPS), FTY720 pretreated LPS-induced ALI group (FTY720 + LPS), FTY720 and NC siRNA-treated LPS-induced ALI group

(FTY720 + LPS + si-NC), and FTY720 and PP2A siRNA-treated LPS-induced ALI group (FTY720 + LPS + si-PP2A). Acute lung injury was induced by intratracheal instillation of LPS (5 mg/kg, Catalog number: L2880, Sigma Company, USA) for 24 hours. Control mice received an equal volume of PBS. Mice in the FTY720 + LPS group were intraperitoneally injected with 0.5 mg/kg FTY720 (Catalog number: 10006292-10, Cayman Company, USA) [14,15] 30 min prior to LPS administration. Mice in the FTY720 + LPS + si-NC group were intraperitoneally injected with FTY720 prior to LPS administration, and then NC siRNA (40 μg/ml, Guangzhou RiboBio Co., Ltd., China) was instilled into the trachea after LPS administration. Mice in the FTY720 + LPS + si-PP2A group were intraperitoneally injected with FTY720 prior to LPS administration, and then PP2A siRNA (40 μg/ml, Guangzhou RiboBio Co., Ltd., China) was instilled into the trachea after LPS administration.

Mice were euthanized 24 h after LPS administration. Bronchoalveolar lavage (BAL) was performed via the left lung. Cell pellets were resuspended for total cell counting using a hemocytometer. The superior lobe of the right lung was collected for histological analysis, the middle lobe for wet-to-dry (W/D) weight determination, and the inferior lobe was snap-frozen in liquid nitrogen and stored at −80 °C until used. In this study, a complete blind assessment was conducted on all results.

Lung wet/dry (W/D) weight ratios

The middle lobe of the right lung was excised and immediately weighed to obtain the wet weight, and dried at 80℃ for 24 h to obtain the dry weight.

Histologic examination

The superior lobe of the right lung was collected, embedded in paraffin wax and

sectioned (3 mm thickness). Sections were stained with hematoxylin-eosin (H&E) and imaged by light microscope (Olympus Optical, Tokyo, Japan). Lung injury was determined by using the semi-quantitative scoring system assessing alveolar congestion or hemorrhage, edema, neutrophil infiltration, and alveolar wall thickening/hyaline membrane formation. Each parameter was scored from 0 (absent) to 4 (severe), and the total lung injury score was calculated as the sum of all parameters.

Survival status

To observe the effects of FTY720 and si-PP2A on the survival of LPS-induced ALI mice, the survival status after 7 days of LPS instillation was observed. Each group consisted of 10 mice, and the observation time points were 6 h, 24 h, 48 h, and 7 days after instillation.

Cell culture

RAW 264.7 cells were cultured in Dulbecco's Modified Eagle's Medium (DMEM) supplemented with 10% fetal bovine serum at 37℃ and 5% CO_2.

Cells were divided into 4 groups: control group (Con), treated with DMEM alone; LPS group (LPS): treated with LPS (100 ng/mL) [16] for 12 h; FTY 720 group (FTY 720): treated with FTY 720 (8 μM) [17] for 6 h; FTY 720 + LPS group (FTY 720 + LPS): treated with FTY 720 (8 μM) for 6 h followed by LPS (100 ng/mL) for 12 h. Culture supernatants were collected for cytokine measurements.

PP2A activity assay

PP2A activity was determined using the PP2A immunoprecipitation phosphatase assay kit (Catalog number: 17-313, Merck Millipore, Darmstadt, Germany) according to the manufacturer’s instructions.

Cytokine measurements

Levels of TNF-α (Catalog number: MTA00B), IL-1β (Catalog number: MLB00C), and IL-6 (Catalog number: M6000B) in cell culture supernatants and BALF were quantified using ELISA kits (R&D Systems, Minneapolis, MN, USA), respectively, following the manufacturer's instructions.

Real-time RT-PCR

Total RNA was extracted using the RNeasy Mini Kit (Catalog number: 74104, Qiagen Australia, Doncaster, VIC, Australia). 1 μg RNA was reverse-transcribed into cDNA using a Thermo Scientific Revert Aid First Strand cDNA Synthesis Kit (Catalog number: K1622, Thermo Scientific, USA) according to the manufacturer's protocol. Quantitative real-time PCR was performed using a SYBR PCR master kit (Catalog number: QPK-201, Takara, China). TTP mRNA level was scaled to β-actin. The gene-specific primers used in Real-time RT-PCR are: TTP (Forward primer:5'- GGTACCCCAG GCTGGCTTT -3' and Reverse primer: 5'- ACCTGTAACCCCAGAACTTGGA -3'); β-actin (Forward primer:5' -GCACCACACCTTCTACAATGAGC- 3' and Reverse primer: 5' -TCGTTGCCAATAGTGATGACC -3'). All primers were synthesized by Sangon Biotech (Shanghai) Co., Ltd. The relative gene expression was calculated using $2^{-(\Delta\Delta Ct)}$.

Western blot analysis

The concentration of protein was determined using a BCA protein detection kit (Catalog number: P0012S, Beyotime, China). 40 μg proteins were separated on denatured 12% polyacrylamide gel, transferred to a polyvinylidene fluoride membrane, and sealed with washing buffer solution. Blots were blocked in 5% non-fat dry milk, incubated with primary antibody overnight at 4℃, washed, incubated with secondary antibody for 1 hour

at room temperature, washed, and developed with Enhanced chemiluminescence (ECL, Catalog number: WBKLS0500, Millipore Corp, Bedford, Massachusetts). β-actin was used as a loading control. Primary antibodies (dilution ratio, vendor) were: anti-PP2A subunit antibodies (Catalog #2038, 1: 1000, cell signaling technology, USA), phosphate-p38MAPK (Thr 180/Tyr 182) (Catalog #9211, 1: 1000, cell signaling technology), total p38MAPK (Catalog #9212, 1: 1000, cell signaling technology), and TTP(Catalog #71632, 1: 1000, cell signaling technology). The secondary antibody was HRP-linked goat anti-rabbit IgG (Catalog #7074, 1:3000, Cell Signaling Technology).

Statistical analysis

The statistical analysis was performed in SPSS 26 (IBM SPSS Statistics) and graphs were made in Prism 10.1.2 (GraphPad Software, Inc.). The normality was assessed using the Shapiro-Wilk test. All data from the three independent experiments that conform to a normal distribution are presented as means ± standard deviation (SD); statistical analysis was performed using one-way ANOVA followed by Tukey post hoc test. An analysis of survival status was conducted using the Kaplan-Meier curve. $p < 0.05$ was considered statistically significant.

3. Results

FTY720 attenuates LPS-induced acute lung injury

Intratracheal administration of LPS is a well-established clinically relevant model of acute lung injury (ALI). Histological examination of lung sections revealed that LPS administration resulted in severe disruption of pulmonary architecture, characterized by alveolar collapse, marked thickening of alveolar septa, intra-alveolar hemorrhage, and extensive infiltration of inflammatory cells. In contrast, lung sections from mice

pretreated with FTY720 exhibited substantially preserved alveolar architecture and markedly attenuated inflammatory lesions,while the treatment with PP2A siRNA blocked the effect of FTY720 in alleviating LPS-induced acute lung injury (Figure 1A). Lung injury scores confirmed these histopathological findings. Semi-quantitative lung injury scores were significantly increased following LPS exposure compared with control mice (11.09 ± 0.81 vs. 2.67 ± 0.43), whereas FTY720 pretreatment significantly reduced lung injury scores (7.22 ± 0.78 vs. LPS). However, the treatment with PP2A siRNA blocked the reduction in lung injury scores caused by FTY720 (LPS + FTY720 + si-NC, 7.20 ± 0.83 vs. LPS + FTY720 + si-PP2A, 10.62 ± 0.88) (Figure 1B). Moreover, pulmonary edema, assessed by the lung wet-to-dry (W/D) weight ratio, was markedly elevated in LPS-treated mice and was significantly attenuated by FTY720 pretreatment (FTY720 +LPS group, 5.63 ±0.32; LPS group, 6.79±0.53). However, the treatment with PP2A siRNA blocked the reduction in lung W/D weight ratio caused by FTY720 (LPS + FTY720 + si-NC, 5.72 ± 0.39 vs. LPS + FTY720 + si-PP2A, 6.62 ± 0.48) (Figure 1C). Together, these data demonstrated that FTY720 confers significant protection against LPS-induced acute lung injury by preserving lung structural integrity and reducing pulmonary edema.

FTY720 mitigates LPS-induced pulmonary inflammation

Because excessive inflammation is a central driver of LPS-induced lung injury, we assessed pulmonary inflammation by analyzing bronchoalveolar lavage fluid (BALF). LPS administration triggered a robust inflammatory reaction, evidenced by a marked increase in total leukocyte counts (14.33 ± 3.26 vs. 2.62 ± 0.25 in controls) and robust neutrophil accumulation (9.57 ± 1.26; vs. 1.52 ± 0.19 in controls). Notably, pretreatment

with FTY720 significantly reduced both total inflammatory cell recruitment and neutrophil infiltration. However, the treatment with PP2A siRNA blocked the increase in total leukocyte counts and neutrophil accumulation caused by FTY720 (Figure 2A and 2B). Consistent with these cellular changes, levels of the pro-inflammatory cytokines TNF-α, IL-1β and IL-6 in BALF were remarkably elevated in the LPS group relative to the control group. FTY720 pretreatment significantly reduced the concentrations of all three cytokines. However, the treatment with PP2A siRNA blocked the reduction in TNF-α, IL-1β, and IL-6 caused by FTY720 (Figure 2C-E), indicating effective suppression of the LPS-induced inflammatory cascade. Collectively, these findings demonstrate that FTY720 markedly mitigates LPS-induced pulmonary inflammation *in vivo*, providing a mechanistic basis for the protective effects against acute lung injury.

FTY720 restores PP2A activity in LPS-treated lungs

Given the established role of protein phosphatase 2A (PP2A) in inflammatory signaling, we examined whether PP2A phosphatase activity is altered during LPS-induced ALI. Although the protein expression of the PP2A catalytic subunit (PP2A-C) remained unchanged in the Con group, LPS group, and FTY720 + LPS group, the PP2A expression in the LPS + FTY720 + si-PP2A group was decreased, compared with the LPS + FTY720 + si-NC group (Figure 3A), PP2A phosphatase activity was significantly reduced in lung tissues from LPS-induced mice compared with controls. Notably, FTY720 pretreatment significantly restored PP2A phosphatase activity in LPS-exposed lungs. Compared with the LPS + FTY720 + si-NC group, the PP2A phosphatase activity in lung tissue of the LPS + FTY720 + si-PP2A group was reduced (Figure 3B). These results indicate that PP2A dysfunction in acute lung injury is driven by impaired phosphatase activity rather

than altered protein abundance, and that FTY720 exerts the protective effect by functionally reactivating PP2A.

Activation of PP2A suppresses phosphorylation of p38MAPK and TTP in LPS-treated lungs

To elucidate the downstream signaling events associated with PP2A activation, we next examined the phosphorylation status of p38 MAPK in lung tissue lysates (Figures 4A and 4B). Western blot analysis revealed that LPS exposure led to a marked increase in p38 MAPK phosphorylation in lung tissues compared with control mice. In contrast, pretreatment with FTY720 significantly attenuated LPS-induced p38MAPK phosphorylation, demonstrating effective suppression of this inflammatory signaling cascade. Compared with the LPS + FTY720 + si-NC group, the p38MAPK phosphorylation level in the LPS + FTY720 + si-PP2A group was increased. Given that TTP is a critical downstream effector of PP2A signaling and that the mRNA-destabilizing activity of TTP is tightly regulated by phosphorylation status, we further assessed TTP phosphorylation dynamics *in vivo*. LPS administration induced a pronounced increase in phosphorylated TTP (approximately a 4.5-fold elevation relative to control lungs). At the same time, unphosphorylated (active) TTP was only modestly increased (approximately 1.8-fold relative to control lungs). Notably, FTY720 pretreatment markedly reversed LPS-induced TTP phosphorylation and increased the level of unphosphorylated TTP to approximately 2.6-fold relative to control. Compared with the LPS + FTY720 + si-NC group, the TTP phosphorylation level in the LPS + FTY720 + si-PP2A group was increased. Taken together, these results demonstrate that FTY720-mediated activation of PP2A suppresses p38 MAPK signaling and shifts the phosphorylation balance of TTP

from an inactive, phosphorylated state toward an active, unphosphorylated form in vivo.

Survival status of FTY720-treated LPS-induced lung injury mice

We observed the survival status of mice within 7 days of LPS treatment and analyzed the survival using a K-M curve. The results showed (Figure 5) that the survival of LPS-treated mice was reduced, and FTY720 treatment improved the survival of LPS-treated mice. Compared with the LPS + FTY720 + si-NC group, the survival of mice in the LPS + FTY720 + si-PP2A group was reduced.

FTY720 activates PP2A and restrains inflammatory cytokine production in macrophages

To validate the central role of PP2A in mediating the anti-inflammatory effects of FTY720 at the cellular level, RAW264.7 macrophages were employed as an in vitro model of LPS-induced inflammation. Consistent with *in vivo* observations, LPS stimulation significantly reduced PP2A phosphatase activity without altering PP2A-C protein expression. Treatment with FTY720 alone enhanced PP2A activity, and pretreatment with FTY720 effectively restored PP2A activity in LPS-stimulated macrophages (Figures 6A and 6B). Functionally, LPS exposure markedly increased the secretion of TNF-α, IL-1β, and IL-6 into the culture medium, whereas FTY720 pretreatment significantly suppressed the production of all three cytokines (Figures 6C–E). These results indicate that FTY720-mediated PP2A activation exerts potent anti-inflammatory effects in macrophages.

FTY720 modulates TTP phosphorylation to suppress inflammation in macrophages

To further determine whether TTP phosphorylation mediates macrophage inflammatory activation, we examined the effects of FTY720 on TTP expression and phosphorylation

status in RAW264.7 cells. Quantitative RT-PCR analysis revealed that LPS stimulation significantly increased TTP mRNA expression in RAW264.7 cells. However, FTY720 pretreatment did not alter either basal or LPS-induced TTP transcription (Figure 7A), indicating that FTY720 regulates TTP predominantly at the post-translational level. Western blot analysis demonstrated that LPS robustly induced phosphorylation of p38 MAPK and TTP, whereas FTY720 pretreatment significantly attenuated phosphorylation of both proteins. Importantly, the level of unphosphorylated TTP was markedly increased in FTY720-pretreated, LPS-stimulated cells compared with LPS treatment alone (Figures 7B and 7C). These findings, together with the *in vivo* data, support a model in TTP-mediated suppression of inflammatory cytokine production.

4. DISCUSSION

This study confirmed that FTY720 exerted significant protective effects in LPS-induced acute lung injury (ALI) by activating the PP2A-TTP signaling axis. Our results indicated that FTY720 treatment preserved lung structural integrity, reduced pulmonary edema, suppressed lung inflammation, and ultimately improved survival rates in LPS-treated mice. Mechanistic studies showed that FTY720-mediated functional activation of PP2A promoted TTP dephosphorylation, thereby inhibiting p38 MAPK signaling and reducing the production of inflammatory cytokines. These findings provide a new theoretical basis for the potential application of FTY720 in ALI treatment.

The inflammatory response played important roles in initiation and maintenance of in ALI, inflammatory cytokines such as TNF-α and IL-1β increase the permeability of pulmonary epithelium, furthermore induced lung tissue damage and accumulation of neutrophils which lead to lung edema[18], IL-6 maintain tissue homeostasis and control

the extent of the inflammatory response, IL-6 is increased in the BALF of patients and higher levels increase mortality, which is identified as one of the biomarkers in monitoring ALI [19]. Recently, the upstream regulation of the transcription of inflammatory cytokines has become a focus of pathogenetic research in ALI/ARDS [20]. A conserved mRNA sequence element, the adenylate- uridylate-rich element (ARE), is found in the majority of these inflammation-associated genes [21,22]. Tristetraprolin (TTP) is a critical anti-inflammatory protein that promotes the decay of ARE-containing mRNAs. Moreover, TTP is widely expressed across various tissues, with particularly high levels observed in the lung[7]. In the present study, LPS stimulation significantly upregulated TTP mRNA and protein expression in both RAW264.7 cells and mouse lung tissue When inflammatory cells are stimulated by LPS, the expression of TTP is rapidly induced, TTP binds to the AREs in the 3' - UTR of mRNAs encoding cytokines such as TNF-α, IL-1β and IL-6, recruiting mRNA-degrading enzymes such as exosome complexes and promoting the degradation of these mRNAs, as a result, the production of inflammatory cytokines is reduced, and the excessive inflammatory response is alleviated.

The main sites of phosphorylation in TTP have been identified by mass spectrometry and site-directed mutation research, and the phosphorylation state of TTP plays an important role in controlling its activity and stability [23]. The activity of TTP is mainly regulated by phosphorylation by protein kinases (such as p38 MAPK and PP2A) in vitro and/or in vivo [24-26]. Protein phosphatase 2A (PP2A) is an important member of serine/theronine protein phosphatase family [27]. PP2A has been demonstrated to interact with p38MAPK and regulate its phosphorylation status in many cell systems. PP2A can dephosphorylate

p38MAPK at the activating phosphorylation sites (Thr180 and Tyr182), resulting in its inactivation [28]. Phosphorylation of TTP at serine residues S52 and S178 in mice, mediated by MAPK-activated protein kinase 2 (MAPK/MK2), inhibits its mRNA destabilizing activity, depending on its phosphorylation state, and PP2A might be therapeutic target to promote the dephosphorylation and activation of TTP. It is reported that PP2A is directly responsible for the dephosphorylation of TTP in vitro and/or in vivo. PP2A activation increases the mRNA destabilizing activity of TTP by dephosphorylating [29,30]. In this study, we found that the activation of PP2A can produce anti-inflammatory effects in LPS-induced RAW 264.7 cells and lung tissues. LPS stimulation increased the expression of TTP mRNA and protein levels, and the pretreatment of PP2A activator regulated the dynamic balance between phosphorylated (inactive) and non-phosphorylated (active) TTP proteins, but did not increase the TTP mRNA level. Dephosphorylation of TTP activated by PP2A leads to the combination of non-phosphorylated TTP with AU-rich components of pro-inflammatory cytokine mRNA, which promotes the degradation of inflammatory cytokine mRNA. It is possible that the molecular mechanism is direct regulation of TTP activity by PP2A and/or indirectly suppressed p38MAPK phosphorylation and promoted dephosphorylation of TTP. PP2A activation shows potential as a method to control TTP activity, could potentially anti-inflammatory therapeutic target in LPS-induced ALI.

Notably, recent studies have further expanded the application scope of FTY720 in pulmonary inflammatory diseases. The inhalable FTY720-nobiletin-PLGA nanoparticle formulation developed by Zhang et al. exhibits good biocompatibility and sustained pharmacological effects in an LPS-induced ALI model. This formulation effectively

blocks the activation of the NF-κB and p38 MAPK pathways by inhibiting the release of cytokines such as IL-6 and TNF-α, thereby reducing lung injury [31]. This inhalable delivery strategy not only reduces the systemic toxicity of FTY720 but also enhances its pulmonary bioavailability, providing new insights for clinical translation. Additionally, in a COPD mouse model, Wang et al. demonstrated that FTY720 reduces IL-1β levels and improves pulmonary inflammation and emphysema by targeting PP2A [32]. This study [32] further revealed that LincR-PPP2R5C influences the ubiquitination degradation of IL-1β by regulating PP2A activity, providing a new molecular mechanism for understanding the central role of PP2A in macrophage inflammatory regulation. These studies collectively support the critical role of the PP2A-TTP axis in pulmonary inflammatory diseases and are consistent with our observations in the ALI model.

This study has several limitations: First, the LPS model cannot fully replicate the multifactorial etiology, temporal evolution, and comorbidity-related immune variations of human ARDS. Given that ALI and cardiovascular diseases share a common pathological basis of "excessive inflammation-oxidative stress," future validation in complex models with comorbidities such as diabetes and hypertension, as well as in aging models, combined with gender-specific analysis, is needed to enhance clinical translational value. Second, the dosing regimen was preventive rather than therapeutic, and subsequent studies should adopt delayed dosing regimens to assess true efficacy. Third, key site mutation experiments for TTP, identification of major cellular targets, and exploration of broader regulatory networks involving PP2A and p38 MAPK/MDM2 were not conducted. Future studies should integrate multi-omics approaches to elucidate the dynamic characteristics of PP2A signaling. Fourth, pharmacological evaluation was insufficient,

lacking pharmacokinetic analysis, sustained efficacy and safety assessments, and positive control groups such as glucocorticoids. Fifth, only male mice were used, limiting the generalizability of the results; future studies should include female animals to assess gender differences.

Based on these limitations, subsequent research should proceed in the following directions: For mechanistic expansion, further elucidate the broader regulatory network of PP2A in inflammation, explore other dephosphorylation targets beyond TTP (such as the MDM2-p53 pathway, which has recently demonstrated regulatory potential for cellular stress and inflammation in the clinical application of MDM2 antagonists [33], and integrate multi-omics analysis to reveal the dynamic characteristics of PP2A signaling. For model optimization, validation should be conducted in ALI models induced by various etiologies (sepsis, viral infections), comorbidity models (diabetes, hypertension), and aging models, incorporating gender-specific analysis. For dosing strategies, inhalable nanoparticle formulations can be drawn on for pulmonary targeted delivery, and the therapeutic window of delayed dosing regimens should be evaluated. For pre-clinical translation assessment, systematic pharmacokinetic/pharmacodynamic studies should be conducted to evaluate long-term cardiovascular safety and infection risk, compare FTY720 head-to-head with glucocorticoids, and explore combination strategies with SGLT2 inhibitors—which exert cardiovascular protection by regulating excessive inflammation and oxidative stress pathways and may have synergistic effects with the PP2A-TTP axis. It is also noteworthy that ALI and cardiovascular diseases share a common pathological basis of "excessive inflammation-oxidative stress." Recent findings suggest that traditional body fat distribution patterns in low-risk female

populations can independently predict cardiac function, and SGLT2 inhibitors exert cardiovascular protection by regulating these pathways [34-37]. Therefore, future studies should validate the efficacy of FTY720 in complex models with comorbidities such as diabetes and hypertension, incorporating gender-specific analysis and exploration of SGLT2-related pathways to promote clinical translation.

In conclusion, this study confirms that FTY720 exerts anti-inflammatory protective effects in LPS-induced ALI through PP2A-mediated TTP dephosphorylation. Unlike FTY720's classical S1P receptor modulation mechanism [38,39], its protective effects in the specific context of ALI primarily depend on the activation of the PP2A pathway. This study links PP2A activation with TTP-mediated post-transcriptional regulation, expanding the understanding of FTY720's pharmacological effects and providing a new theoretical basis for ALI treatment. Although further validation in more complex models, closer-to-clinical dosing regimens, and more comprehensive safety assessments is needed before clinical translation, the PP2A-TTP axis has shown potential as an intervention target for inflammatory lung injury and warrants further in-depth study.

Acknowledgements

This work was supported by the Natural Science Foundation of Shaanxi (2018JM7078).

References

1. Liang D, Liu C, Yang M. Mesenchymal stem cells and their derived exosomes for ALI/ARDS: A promising therapy. Heliyon. Oct 2023;9(10):e20387. doi:10.1016/j.heliyon.2023.e20387

2. Liao J, Liang Y, Liu Z, Xie Q, Zhang JM, Song SY, Huang X, Cao L, Wang Y. Pyroptosis in acute respiratory distress syndrome and pulmonary fibrosis. Biomedicine &

pharmacotherapy = Biomedecine & pharmacotherapie. Aug 2025;189:118286. doi:10.1016/j.biopha.2025.118286

3. Bredeck G, Dobner J, Stahlmecke B, Fomba KW, Herrmann H, Rossi A, Schins RPF. Saharan dust induces NLRP3-dependent inflammatory cytokines in an alveolar air-liquid interface co-culture model. Particle and fibre toxicology. Oct 20 2023;20(1):39. doi:10.1186/s12989-023-00550-w

4. Wu B, Xu MM, Fan C, Feng CL, Lu QK, Lu HM, Xiang CG, Bai F, Wang HY, Wu YW, Tang W. STING inhibitor ameliorates LPS-induced ALI by preventing vascular endothelial cells-mediated immune cells chemotaxis and adhesion. Acta pharmacologica Sinica. Aug 2022;43(8):2055-2066. doi:10.1038/s41401-021-00813-2

5. Ito J, Miyake K, Chiba T, Takahashi K, Uchida Y, Blackshear PJ, Asahara H, Karasuyama H. Tristetraprolin-mediated mRNA destabilization regulates basophil inflammatory responses. Allergology international : official journal of the Japanese Society of Allergology. Apr 2025;74(2):263-273. doi:10.1016/j.alit.2024.10.005

6. Tiedje C, Diaz-Munoz MD, Trulley P, Ahlfors H, Laass K, Blackshear PJ, Turner M, Gaestel M. The RNA-binding protein TTP is a global post-transcriptional regulator of feedback control in inflammation. Nucleic acids research. Sep 6 2016;44(15):7418-7440. doi:10.1093/nar/gkw474

7. Zhang Y, Wang G, Zhang D, Sun X. Resveratrol Ameliorates LPS-induced Acute Lung Injury Mouse Model via Induction of Tristetraprolin. Combinatorial chemistry & high throughput screening. 2023;26(4):838-847. doi:10.2174/1386207325666220601123047

8. Clark AR, Dean JL. The control of inflammation via the phosphorylation and

dephosphorylation of tristetraprolin: a tale of two phosphatases. Biochemical Society transactions. Oct 15 2016;44(5):1321-1337. doi:10.1042/BST20160166

9. Carreno A, Lykke-Andersen J. The Conserved CNOT1 Interaction Motif of Tristetraprolin Regulates ARE-mRNA Decay Independently of the p38 MAPK-MK2 Kinase Pathway. Molecular and cellular biology. Sep 15 2022;42(9):e0005522. doi:10.1128/mcb.00055-22

10. Rahman MM, Rumzhum NN, Morris JC, Clark AR, Verrills NM, Ammit AJ. Basal protein phosphatase 2A activity restrains cytokine expression: role for MAPKs and tristetraprolin. Scientific reports. May 18 2015;5:10063. doi:10.1038/srep10063

11. De Palma RM, Parnham SR, Li Y, Oaks JJ, Peterson YK, Szulc ZM, Roth BM, Xing Y, Ogretmen B. The NMR-based characterization of the FTY720-SET complex reveals an alternative mechanism for the attenuation of the inhibitory SET-PP2A interaction. FASEB journal : official publication of the Federation of American Societies for Experimental Biology. Jun 2019;33(6):7647-7666. doi:10.1096/fj.201802264R

12. Rahman MM, Prunte L, Lebender LF, Patel BS, Gelissen I, Hansbro PM, Morris JC, Clark AR, Verrills NM, Ammit AJ. The phosphorylated form of FTY720 activates PP2A, represses inflammation and is devoid of S1P agonism in A549 lung epithelial cells. Scientific reports. Nov 16 2016;6:37297. doi:10.1038/srep37297

13. Qadri M, ElSayed S, Elsaid KA. Fingolimod Phosphate (FTY720-P) Activates Protein Phosphatase 2A in Human Monocytes and Inhibits Monosodium Urate Crystal-Induced Interleukin-1beta Production. The Journal of pharmacology and experimental therapeutics. Feb 2021;376(2):222-230. doi:10.1124/jpet.120.000321

14. Shi ZA, Yu CX, Wu ZC, Chen CL, Tu FP, Wan Y. The effect of FTY720 at different

doses and time-points on LPS-induced acute lung injury in rats. International immunopharmacology. Oct 2021;99:107972. doi:10.1016/j.intimp.2021.107972

15. Wang L, Sammani S, Moreno-Vinasco L, Letsiou E, Wang T, Camp SM, Bittman R, Garcia JG, Dudek SM. FTY720 (s)-phosphonate preserves sphingosine 1-phosphate receptor 1 expression and exhibits superior barrier protection to FTY720 in acute lung injury. Critical care medicine. Mar 2014;42(3):e189-199. doi:10.1097/CCM.0000000000000097

16. Yamaguchi M, Levy RM. The combination of catechin, baicalin and beta-caryophyllene potentially suppresses the production of inflammatory cytokines in mouse macrophages in vitro. Experimental and therapeutic medicine. May 2019;17(5):4312-4318. doi:10.3892/etm.2019.7452

17. Yu H, Herbert BA, Valerio M, Yarborough L, Hsu LC, Argraves KM. FTY720 inhibited proinflammatory cytokine release and osteoclastogenesis induced by Aggregatibacter actinomycetemcomitans. Lipids in health and disease. Jul 4 2015;14:66. doi:10.1186/s12944-015-0057-7

18. Zhao G, Zhang T, Ma X, Jiang K, Wu H, Qiu C, Guo M, Deng G. Oridonin attenuates the release of pro-inflammatory cytokines in lipopolysaccharide-induced RAW264.7 cells and acute lung injury. Oncotarget. Sep 15 2017;8(40):68153-68164. doi:10.18632/oncotarget.19249

19. Chen C, Shi L, Li Y, Wang X, Yang S. Disease-specific dynamic biomarkers selected by integrating inflammatory mediators with clinical informatics in ARDS patients with severe pneumonia. Cell biology and toxicology. Jun 2016;32(3):169-184. doi:10.1007/s10565-016-9322-4

20. Shen X, He L, Cai W. Role of Lipopolysaccharides in the Inflammation and Pyroptosis of Alveolar Epithelial Cells in Acute Lung Injury and Acute Respiratory Distress Syndrome. Journal of inflammation research. 2024;17:5855-5869. doi:10.2147/JIR.S479051

21. Beisang D, Bohjanen PR. Perspectives on the ARE as it turns 25 years old. Wiley interdisciplinary reviews RNA. Sep-Oct 2012;3(5):719-731. doi:10.1002/wrna.1125

22. Kovarik P, Bestehorn A, Fesselet J. Conceptual Advances in Control of Inflammation by the RNA-Binding Protein Tristetraprolin. Frontiers in immunology. 2021;12:751313. doi:10.3389/fimmu.2021.751313

23. Pommier A, Bleuse S, Deletang K, Varilh J, Nadaud M, Boisguerin P, Bourdin A, Taulan-Cadars M. The RNA-Binding Protein Tristetraprolin Contributes to CFTR mRNA Stability in Cystic Fibrosis. American journal of respiratory cell and molecular biology. Mar 2025;72(3):320-331. doi:10.1165/rcmb.2023-0209OC

24. Prabhala P, Bunge K, Ge Q, Ammit AJ. Corticosteroid-Induced MKP-1 Represses Pro-Inflammatory Cytokine Secretion by Enhancing Activity of Tristetraprolin (TTP) in ASM Cells. Journal of cellular physiology. Oct 2016;231(10):2153-2158. doi:10.1002/jcp.25327

25. Rezcallah MC, Al-Mazi T, Ammit AJ. Cataloguing the phosphorylation sites of tristetraprolin (TTP): Functional implications for inflammatory diseases. Cellular signalling. Feb 2021;78:109868. doi:10.1016/j.cellsig.2020.109868

26. Scinicariello S, Soderholm A, Schafer M, Shulkina A, Schwartz I, Hacker K, Gogova R, Kalis R, Froussios K, Budroni V, Bestehorn A, Clausen T, Kovarik P, Zuber J, Versteeg GA. HUWE1 controls tristetraprolin proteasomal degradation by regulating its

phosphorylation. eLife. Mar 24 2023;12doi:10.7554/eLife.83159

27. Ivovic D, Kabelikova P, Jurkovicova D. Unraveling the complexity: A comprehensive analysis of the PP2A in cancer and its potential for novel targeted therapies. Neoplasma. Aug 2023;70(4):485-499. doi:10.4149/neo_2023_230806N411

28. Zhang L, Ma P, Guan Q, Meng L, Su L, Wang L, Zhao J, Ji S. Protein phosphatase 2A regulates the p38 signaling pathway to affect the migration of astrocytes. Molecular medicine reports. Nov 2018;18(5):4328-4334. doi:10.3892/mmr.2018.9425

29. Park SY, Jeong YJ, Lee KS, Park JY, Park J, Tesh VL, Lee MS. Shiga Toxins Produced by Enterohaemorrhagic Escherichia coli Induce Inflammation in Toxin-Sensitive Cells through the p38 MAPK/MK2/Tristetraprolin Signaling Pathway. Journal of microbiology and biotechnology. Dec 28 2024;34(12):2439-2449. doi:10.4014/jmb.2410.10016

30. Rahman MM, Rumzhum NN, Hansbro PM, Morris JC, Clark AR, Verrills NM, Ammit AJ. Activating protein phosphatase 2A (PP2A) enhances tristetraprolin (TTP) anti-inflammatory function in A549 lung epithelial cells. Cellular signalling. Apr 2016;28(4):325-334. doi:10.1016/j.cellsig.2016.01.009

31. Zhang HH, Kuo WS, Tu PY, Lee CT, Wang HC, Huang YT, Shen MC, Lin TS, Su PL, Tsai JS, Pan MH, Lin CC, Wu PC. Enhancing Lung Recovery: Inhaled Poly(lactic-co-glycolic) Acid Encapsulating FTY720 and Nobiletin for Lipopolysaccharide-Induced Lung Injury, with Advanced Inhalation Tower Technology. ACS nano. Mar 4 2025;19(8):7634-7649. doi:10.1021/acsnano.3c12532

32. Wang M, Zhu M, Jia X, Wu J, Yuan Q, Xu T, Wang Z, Huang M, Ji N, Zhang M. LincR-PPP2R5C regulates IL-1beta ubiquitination in macrophages and promotes airway

inflammation and emphysema in a murine model of COPD. International immunopharmacology. Sep 30 2024;139:112680. doi:10.1016/j.intimp.2024.112680

33. Almukram AM, Al-hussaniy HA, Jabarah MA, Al-Abdeen SH. MDM2 Antagonists and p53-Targeting Therapies in Cancer: Clinical Applications, Adverse Effects, and Resistance Mechanisms. Medical and Pharmaceutical Journal. 2025 Apr 4;4(1):47-63. DOI: https://doi.org/10.55940/medphar202567

34. Caturano A, Rocco M, Tagliaferri G, Piacevole A, Nilo D, Di Lorenzo G, Iadicicco I, Donnarumma M, Galiero R, Acierno C, Sardu C, Russo V, Vetrano E, Conte C, Marfella R, Rinaldi L, Sasso FC. Oxidative Stress and Cardiovascular Complications in Type 2 Diabetes: From Pathophysiology to Lifestyle Modifications. Antioxidants. Jan 9 2025;14(1)doi:10.3390/antiox14010072

35. Sardu C, Pieretti G, D'Onofrio N, Ciccarelli F, Paolisso P, Passavanti MB, Marfella R, Cioffi M, Mone P, Dalise AM, Ferraraccio F, Panarese I, Gambardella A, Passariello N, Rizzo MR, Balestrieri ML, Nicoletti G, Barbieri M. Inflammatory Cytokines and SIRT1 Levels in Subcutaneous Abdominal Fat: Relationship With Cardiac Performance in Overweight Pre-diabetics Patients. Frontiers in physiology. 2018;9:1030. doi:10.3389/fphys.2018.01030

36. Sardu C, Gatta G, Pieretti G, Onofrio N, Balestrieri ML, Scisciola L, Cappabianca S, Ferraro G, Nicoletti GF, Signoriello G, Sportiello L, Savarese G, Melchionna M, Ciccarelli F, La Forgia D, Paolisso G, Marfella R. SGLT2 breast expression could affect the cardiovascular performance in pre-menopausal women with fatty vs. non fatty breast via over-inflammation and sirtuins' down regulation. European journal of internal medicine. Jul 2023;113:57-68. doi:10.1016/j.ejim.2023.04.012

37. Sardu C, Gatta G, Pieretti G, Viola L, Sacra C, Di Grezia G, Musto L, Minelli S, La Forgia D, Capodieci M, Galiano A, Vestito A, De Lisio A, Pafundi PC, Sasso FC, Cappabianca S, Nicoletti G, Paolisso G, Marfella R. Pre-Menopausal Breast Fat Density Might Predict MACE During 10 Years of Follow-Up: The BRECARD Study. JACC Cardiovascular imaging. Feb 2021;14(2):426-438. doi:10.1016/j.jcmg.2020.08.028

38. Liu J, Zhang L, Liu L, Wu T, Wang L, Han Q. The potential capacities of FTY720: Novel therapeutic functions, targets, and mechanisms against diseases. European journal of medicinal chemistry. Jun 5 2025;290:117508. doi:10.1016/j.ejmech.2025.117508

39. Coyle PK, Freedman MS, Cohen BA, Cree BAC, Markowitz CE. Sphingosine 1-phosphate receptor modulators in multiple sclerosis treatment: A practical review. Annals of clinical and translational neurology. Apr 2024;11(4):842-855. doi:10.1002/acn3.52017

Figure Legend:

Figure1. FTY720 improved pathologic changes in lung tissues in LPS-induced ALI in mice. Each group of mice was attacked with PBS, LPS, FTY 720 or PP2A siRNA. Samples of lung tissue were collected and analyzed 24 hours after intratracheal administration of LPS. (A) Lung histopathological changes were assayed by hematoxylin-eosin staining (×400); (B) The lung injury score was expressed as the total scores of four independent parameters: alveolar congestion or hemorrhage, edema, neutrophil infiltration, alveolar wall thickening/hyaline membrane formation; (C) The ratio of wet to dry weight of the lung was also measured. Results are presented as mean ± standard deviation (SD) (n = 10 mice per group). Con: control group; LPS: LPS-induced

ALI group; FTY720 + LPS: FTY720 pretreatment LPS-induced ALI group; FTY720 + LPS + si-NC: FTY720 and NC siRNA-treated LPS-induced ALI group; FTY720 + LPS + si-PP2A: FTY720 and PP2A siRNA-treated LPS-induced ALI group.

Figure 2. FTY720 attenuated LPS-induced lung inflammation. (A) Total cell counts in the BALF; (B) Neutrophils in the BALF; (C)Levels of TNF-α in BALF were determined by ELISA; (D) Levels of IL-1β in BALF were determined by ELISA; (E) Levels of IL-6 in BALF were determined by ELISA. Results are presented as mean ± standard deviation (SD) (n = 10 mice per group). Con: control group; LPS: LPS-induced ALI group; FTY720 + LPS: FTY720 pretreatment LPS-induced ALI group; FTY720 + LPS + si-NC: FTY720 and NC siRNA-treated LPS-induced ALI group; FTY720 + LPS + si-PP2A: FTY720 and PP2A siRNA-treated LPS-induced ALI group.

Figure 3. Effects of FTY720 on PP2A phosphatase activity in the lungs of mice in LPS-induced ALI. (A)Western blotting analyses of catalytic subunit of PP2A (PP2A-C) level in the lungs of mice and its quantification analysis; (B) PP2A phosphatase activity tested by a commercial assay. Results are presented as mean ± standard deviation (SD) (n = 10 mice per group). Con: control group; LPS: LPS-induced ALI group; FTY720 + LPS: FTY720 pretreatment LPS-induced ALI group; FTY720 + LPS + si-NC: FTY720 and NC siRNA-treated LPS-induced ALI group; FTY720 + LPS + si-PP2A: FTY720 and PP2A siRNA-treated LPS-induced ALI group.

Figure 4. Effects of FTY720 on phosphorylation of p38MAPK and TTP in LPS-treated

mice lungs. (A) The representative western blot of phosphorylated p38MAPK level compared to total p38MAPK in mice lungs and its quantification analysis; (B) The representative western blot of TTP protein level in mice lung and its quantification analysis (β-actin as loading control), bands at higher molecular weight indicate phosphorylated TTP, while lower bands are unphosphorylated. Results are presented as mean ± standard deviation (SD) (n = 10 mice per group). Con: control group; LPS: LPS-induced ALI group; FTY720 + LPS: FTY720 pretreatment LPS-induced ALI group; FTY720 + LPS + si-NC: FTY720 and NC siRNA-treated LPS-induced ALI group; FTY720 + LPS + si-PP2A: FTY720 and PP2A siRNA-treated LPS-induced ALI group.

Figure 5. Effect of FTY720 on the survival of LPS-treated mice. Kaplan-Meier curve analysis of the survival of mice in each group, n = 10 mice per group. Con: control group; LPS: LPS-induced ALI group; FTY720 + LPS: FTY720 pretreatment LPS-induced ALI group; FTY720 + LPS + si-NC: FTY720 and NC siRNA-treated LPS-induced ALI group; FTY720 + LPS + si-PP2A: FTY720 and PP2A siRNA-treated LPS-induced ALI group.

Figure 6. Effect of FTY720 on phosphatase activity, PP2A, and inflammatory cytokines in RAW264.7 cells. (A)Western blotting analyses catalytic subunit of PP2A (PP2A-C) level in RAW264.7 cells and its quantification analysis (β-actin as loading control); (B) PP2A enzymatic activity tested by a commercial assay; (C) Levels of TNF-α in Cell culture media were determined by ELISA; (D) Levels of IL-1β in cell culture media were determined by ELISA; (E) Levels of IL-6 in cell culture media were determined by ELISA. Results are presented as mean ± standard deviation (SD) (n = 3. Repeated three

599 times). Con: control; LPS: LPS-treated group; FTY720: FTY720-treated group; FTY720
600 + LPS: LPS and FTY720 -treated group.
601
602 Figure 7. Effects of FTY720 on phosphorylation of p38MAPK and TTP in RAW264.7
603 cells. (A) Real-time RT-PCR analysis of TTP mRNA in RAW264.7 cells (β-actin mRNA
604 was used as the internal reference gene, and the relative gene expression was calculated
605 using $2^{-(\Delta\Delta Ct)}$); (B) Representative western blot bands for phosphorylated p38MAPK
606 level and total p38 MAPK in RAW264.7 cells. Densitometric analysis was performed to
607 obtain the relative level of phosphorylated p38MAPK with total p38 MAPK; (C)
608 Representative western blot of TTP protein levels in RAW264.7 cells and its
609 quantification analysis (β-actin as a loading control), the band at higher molecular weight
610 indicate phosphorylated TTP, while the lower band is unphosphorylated. Results are
611 presented as mean ± standard deviation (SD) (n = 3. Repeated three times). Con: control;
612 LPS: LPS-treated group; FTY720: FTY720-treated group; FTY720 + LPS: LPS and
613 FTY720 -treated group.
614

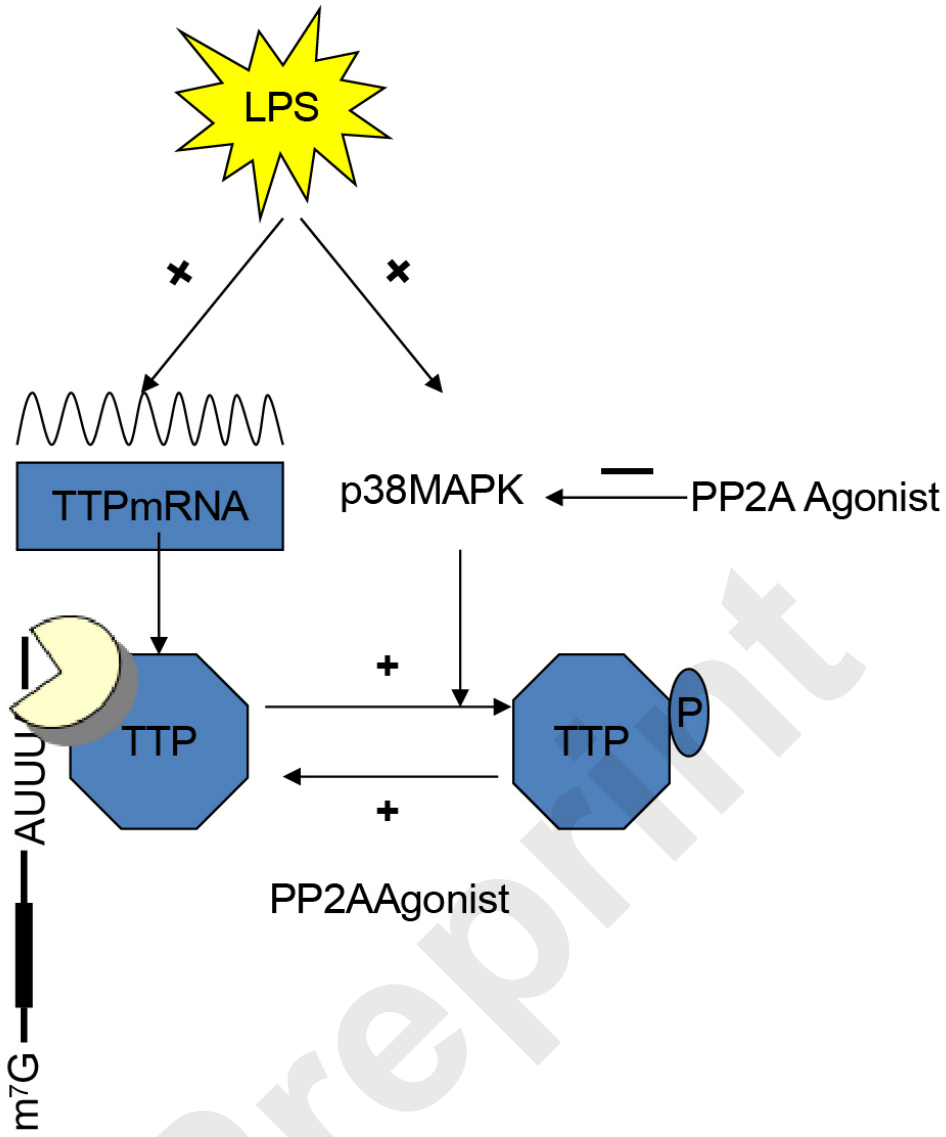
LPS
TTPmRNA
p38MAPK
PP2A Agonist
TTP
TTP
P
AUUU
m7G
PP2AAgonist

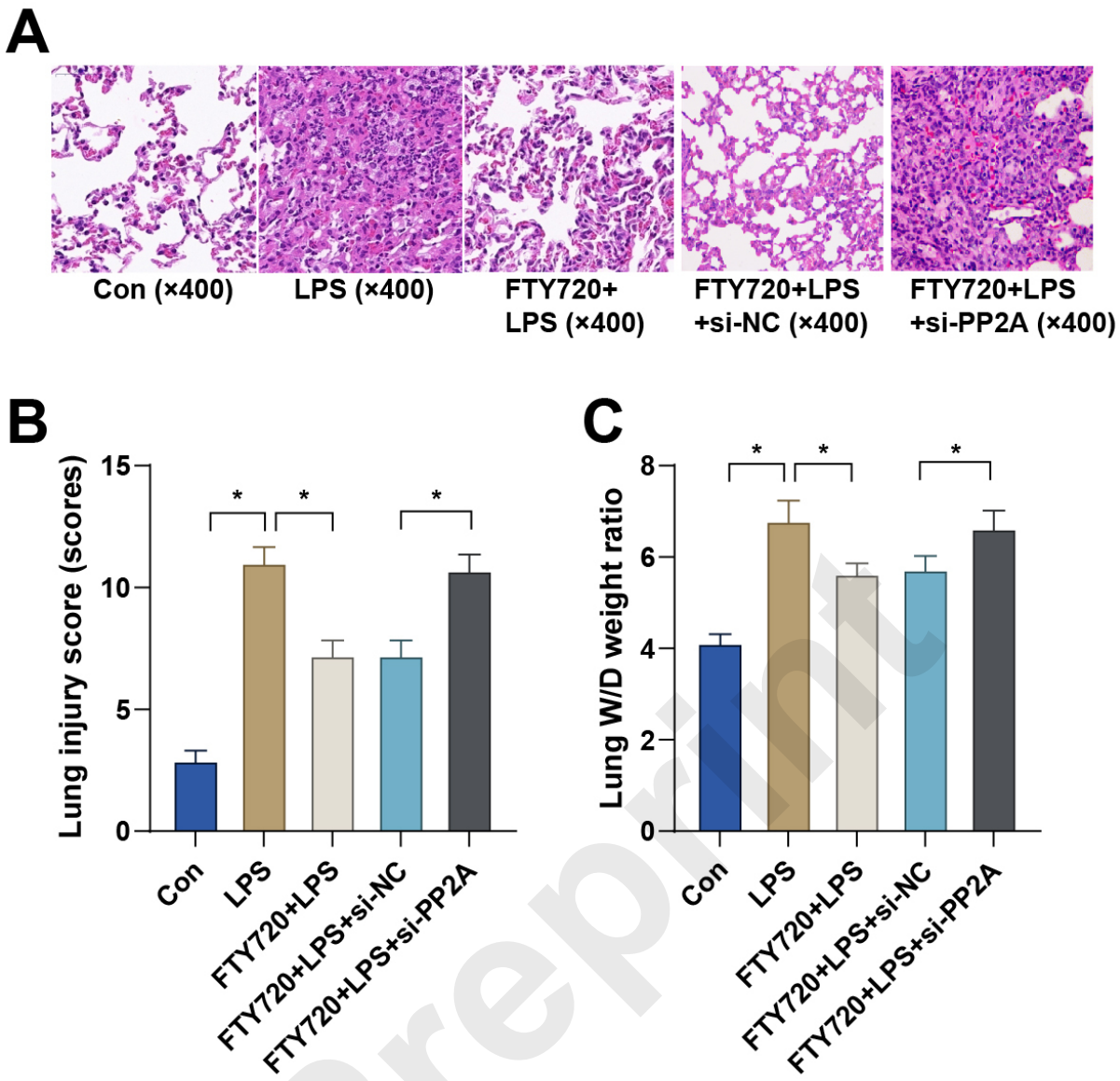

Figure1. FTY720 improved pathologic changes in lung tissues in LPS-induced ALI in mice.

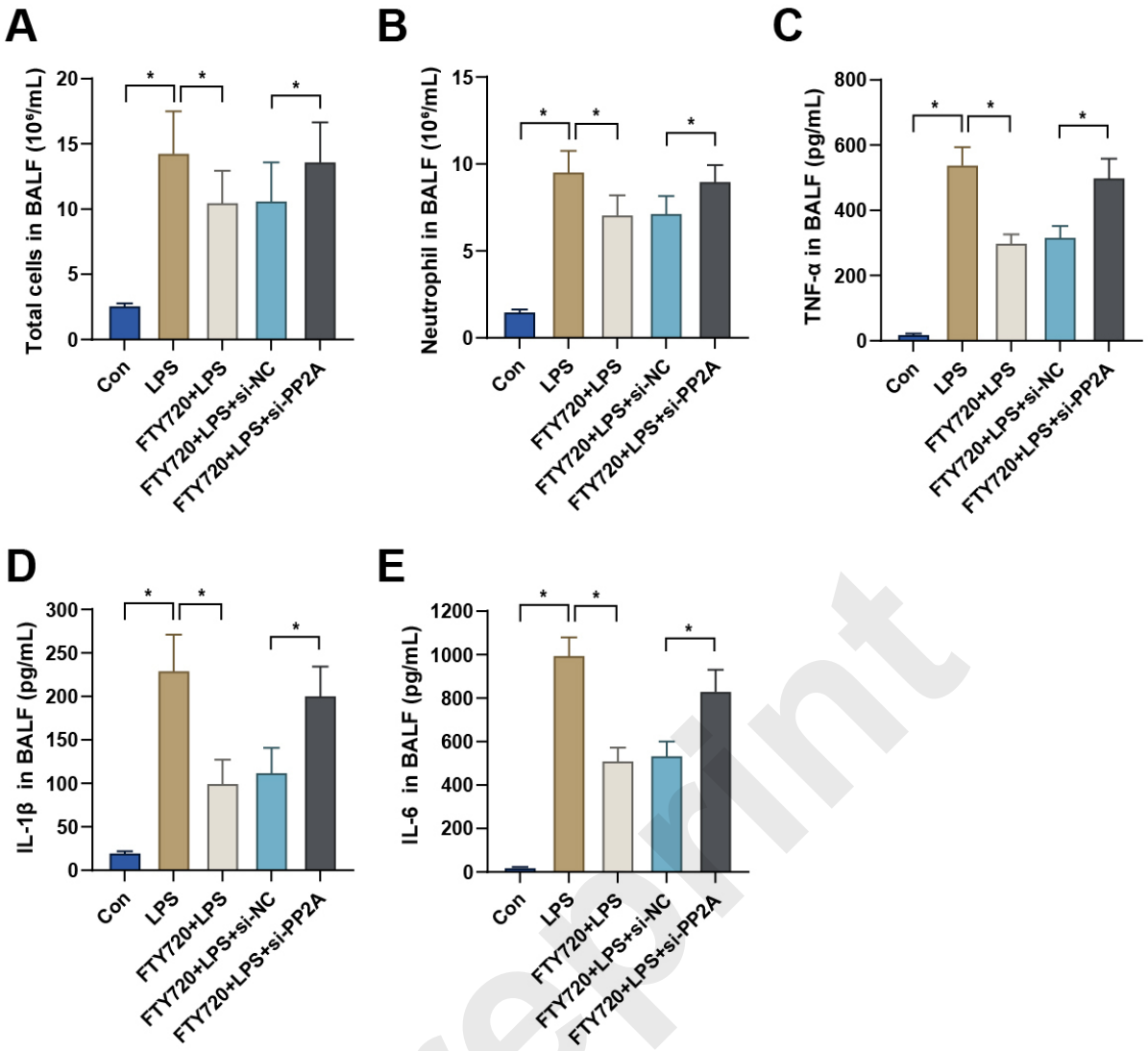

Figure 2. FTY720 attenuated LPS-induced lung inflammation.

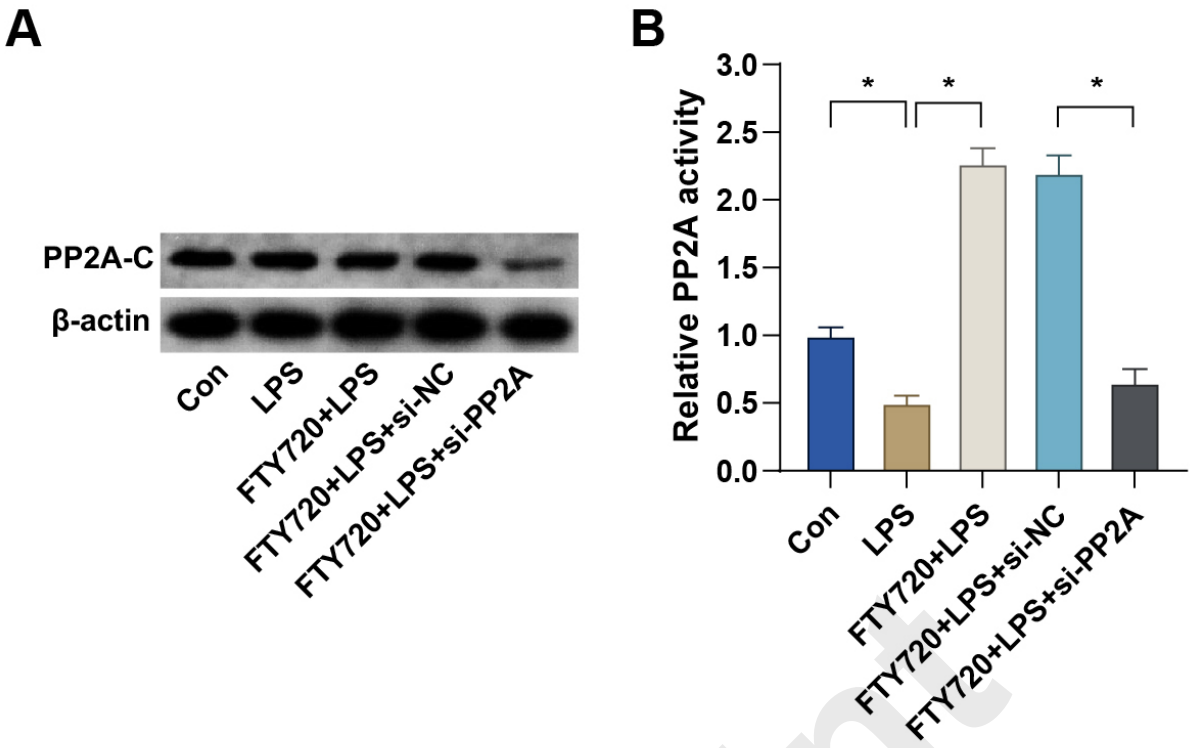

Figure 3. Effects of FTY720 on PP2A phosphatase activity in the lungs of mice in LPS-induced ALI.

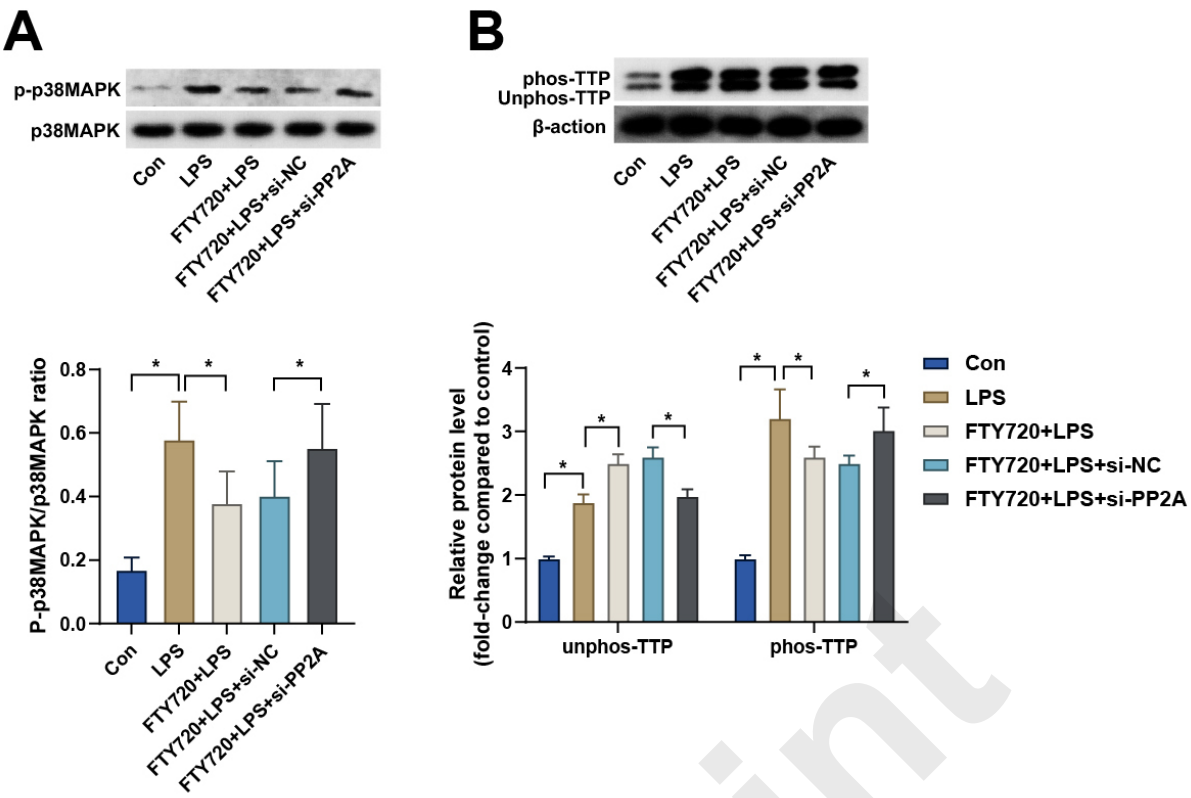

Figure 4. Effects of FTY720 on phosphorylation of p38MAPK and TTP in LPS-treated mice lungs.

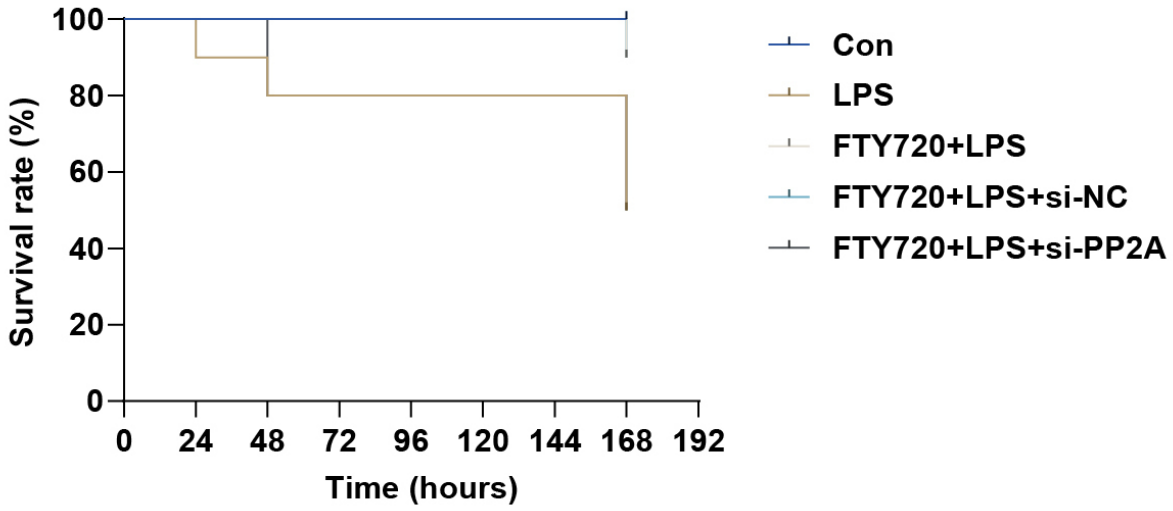

Figure 5. Effect of FTY720 on the survival of LPS-treated mice. Kaplan-Meier curve analysis of the survival of mice in each group, n = 10 mice per group.

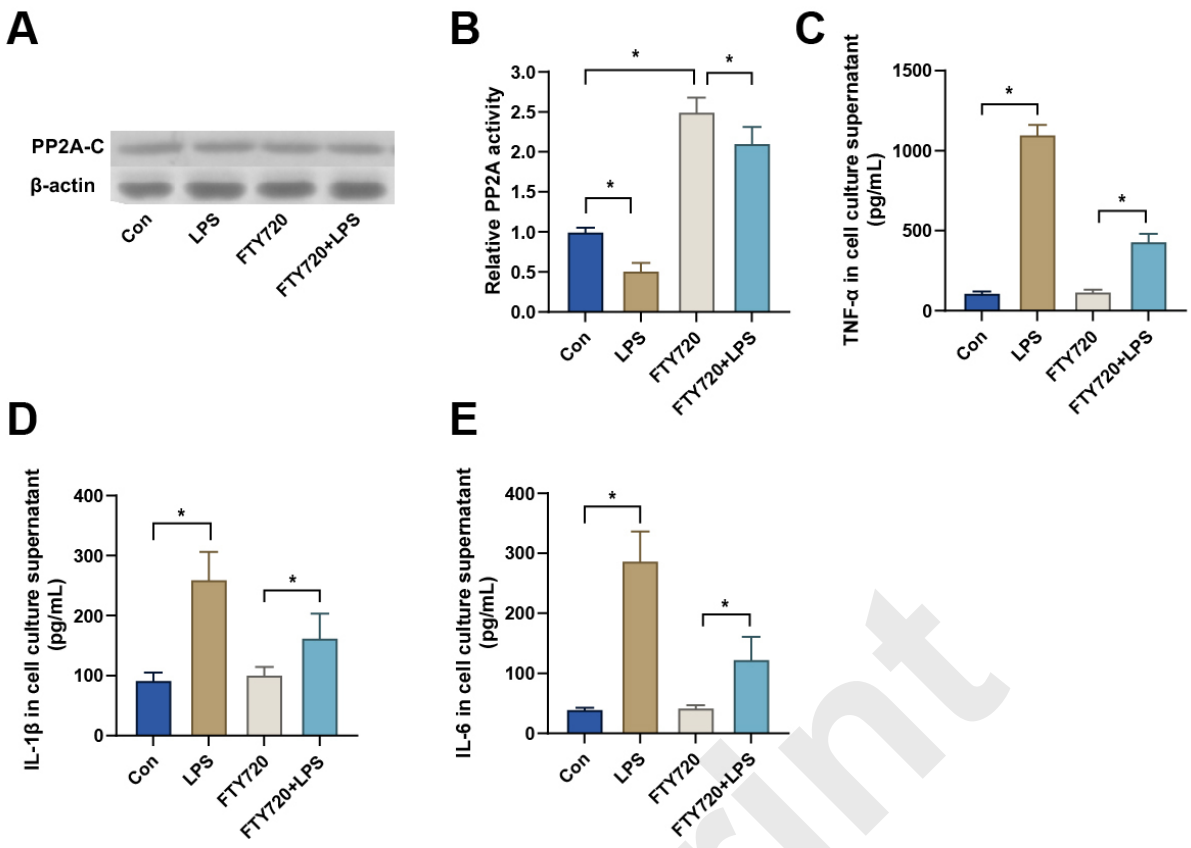

Figure 6. Effect of FTY720 on phosphatase activity, PP2A, and inflammatory cytokines in RAW264.7 cells.

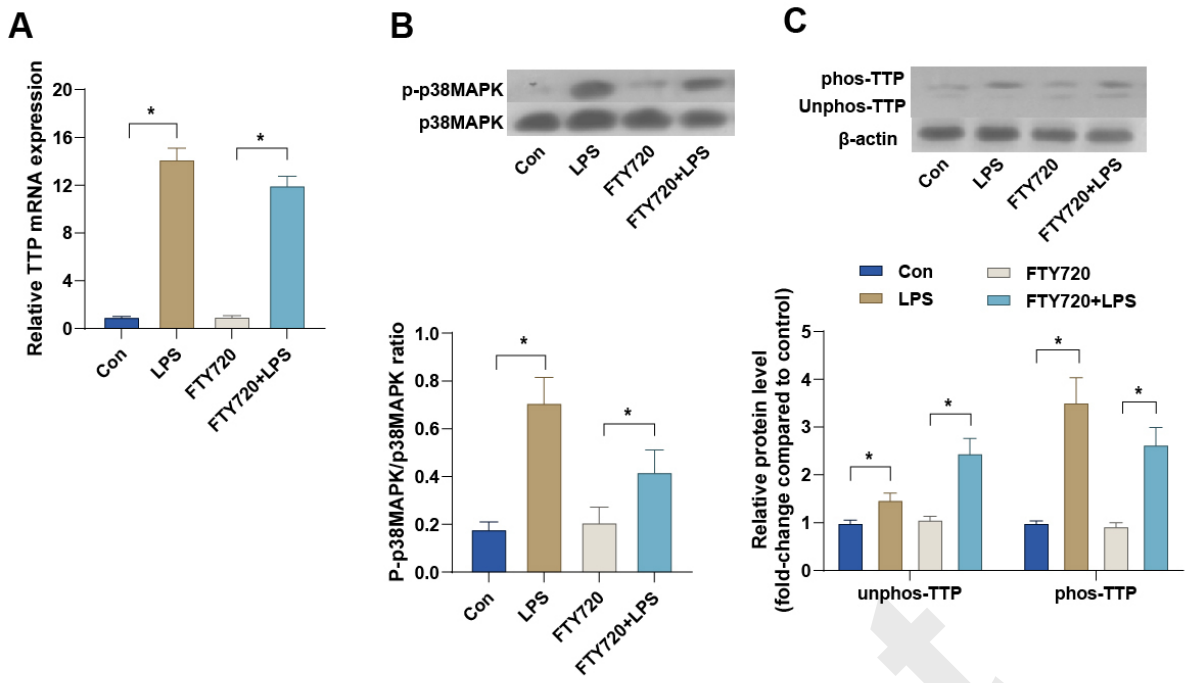

Figure 7. Effects of FTY720 on phosphorylation of p38MAPK and TTP in RAW264.7 cells.